

Important Guidelines On The Finite Element Modelling Of Micropiles

Ahmed Elsaywaf and Hany El Naggar
Dalhousie University, Halifax, Canada
ahmed.elsawwaf@dal.ca; hany.elnaggar@dal.ca

Abstract – This paper highlights essential considerations for FE modeling of pressure-grouted micropiles. To accurately simulate micropile behaviour, it is crucial to consider both its composition and construction method. The use of pressurized grout for micropile construction has a considerable effect on the behaviour of the pile and the surrounding soil. In addition, micropiles generally acquire a high elastic modulus, owing to the high percentage of steel reinforcement adopted. Not considering this installation procedure and/or the high elastic modulus would lead to underestimated predictions of the micropile load capacity. A brief introduction is also given to the Increased K_s Method, which was extensively used in the literature for FE simulation of the effects of the micropile installation process.

Keywords: FE modelling, pressure-grouted micropiles, elastic modulus, Increased K_s Method, PLAXIS

1. Introduction

Micropiles have been used worldwide for deep foundations, underpinning, and in-situ reinforcement since they were developed in the 1950s in Italy [1]. Micropiles are categorized herein as drilled cast-in-place foundations based on the installation method. A micropile is typically constructed by drilling a hole less than 300 mm in diameter, placing steel reinforcement, and applying a grouting procedure with a high pressure to improve the surrounding grout. Casing or drilling fluid (slurry) may be used to support the walls of the hole during the construction. The Federal Highway Administration (FHWA) [2] has published a guideline for the design of micropiles and classified micropiles into four groups (A, B, C, D) based on the method of grouting. The micropile will be classified as Type A if the cement grout is placed under gravity. Type B indicates that cement grout is injected into the hole under a typical pressure of 0.5 to 1 MPa. Type C: the grout is poured first under the gravity head, and after 15–25 min, prior to hardening of the primary grout, cement grout is injected once again at a pressure of at least 1 MPa. The grouting method D is similar to Type C, where additional grout is injected into the micropile shaft after the hardening of the primary grout. However, the grouting operation is carried out along the micropile and at different depths by using a packer.

The use of pressurized grout for micropile construction has a considerable effect on the behaviour of the pile and the surrounding soil [3], [4]. The shaft skin friction increases significantly after a grout injection. Traditional finite element modelling typically treats piles as either bored or low-displacement types. However, this approach is inadequate for micropile problems involving cement grout injection under high pressures, possibly exceeding 1000 kPa. In the literature, few researchers, who did numerical studies on micropiles, tried to consider the numerical consequences of the micropile installation process by increasing the coefficient of lateral earth pressure (K_s) of the soil to account for the increase of radial stresses around the pile [5]–[9]. As an initial phase of a comprehensive research study on different approaches used for FE simulation of micropile installation and loading, the present paper aims to highlight some guidelines on the finite element modelling of pressure-grouted micropiles.

2. Modelling of Micropiles in PLAXIS

2.1. Effects of the installation process

Although micropiles are often constructed by injecting cement grout under high pressure, many practicing engineers do not take into account the FE simulation of the installation process. Either by simply modelling micropiles as embedded beams or even volume tetrahedral elements, PLAXIS will highly underestimate the load capacity of the micropile if the effects of the installation process are not considered in the finite element modelling. For instance, Figure 1 shows the load settlement response of a Type C micropile that was constructed using a grouting pressure of 1.3 MPa [10] versus the numerical results obtained by PLAXIS for the micropile in the same ground conditions without considering the installation process. The

micropile, which had a diameter of 0.165 m and a length of 10 m, was embedded in a soil profile consisting of silty sand and soft silty clay. While it could bear around 1310 kPa at a settlement level of 43.4 mm, the FE results showed that it can only bear around 180 kPa.

Not only do engineers have to consider the installation process in FE modelling, but the interface reduction factor (R_{int}), used to control the friction behaviour of the soil/grout interface, should be in the range of 0.95 to 1.0 to simulate the very rough corrugated surface condition of pressure-grouted micropiles [5], [6], [11].

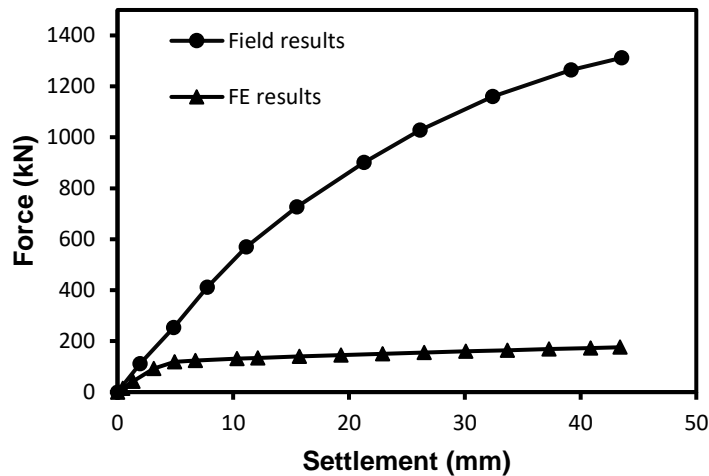


Fig. 1: FE results versus field results obtained by Kyung et al. [10].

2.2. The Increased K_s Method

The easiest method for simulating the radial stress increase due to pile installation is using an increased K_s value (where K_s is the coefficient of lateral earth pressure). This method was used by a number of researchers who investigated the behaviour of micropiles under axial and lateral loads [5]–[9], [12], [13]. In PLAXIS, this method involves two steps. The first is an initial phase in which the initial in situ stress state is developed using the K_o procedure. Here, PLAXIS generates vertical stresses that are in equilibrium with the self-weight of the soil, and horizontal stresses are calculated from the specified value of K_s . After that, in the second step, the pile is installed.

The increased value of K_s may be obtained by back-calculation from a micropile loading test or by direct data from the site using earth pressure cells. Then, in FE modelling, it should be applied to a limited zone of influence around and beneath the micropile, not to the whole soil volume. Alnuaim et al. [5] investigated the performance of micropiled rafts in sand by a numerical model that was calibrated using Centrifuge testing results. They stated that the zone affected by the micropile installation process extends to about $5 D_{mp}$ from the micropile. However, applying the increased value of K_s to a limited distance around the micropile in PLAXIS will generate a stress field that is not in equilibrium, since the K_o procedure does not generate shear stresses. As shown in Figure 2, at the same elevation, the horizontal stress on a soil element inside the zone of influence will be higher than on a soil element outside this zone. Upon generating shear stresses in the soil during a subsequent plastic phase, PLAXIS will redevelop a new stress state, relieving the horizontal stresses in the zone of interest and preventing the achievement of the intended level of lateral stresses.

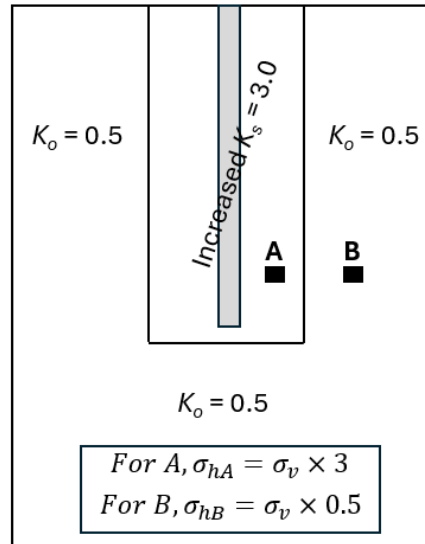


Fig. 2: Non-equilibrium of the stress state developed by the K_o procedure.

In order to overcome the limitation mentioned above, some practicing engineers and researchers apply the increased value of K_s to the whole width of the numerical model. Unfortunately, this will generate an unrealistic stress state around the micropile, where the radial and hoop stresses will be equally increased through the whole width of the soil. Moreover, applying the increased value of K_s to the whole soil width would overestimate the performance of the foundation, especially in micropiled rafts where micropiles are placed under specific areas of the foundation rather than uniformly across the entire raft.

What should be also done in PLAXIS is to apply the increased value of K_s to a limited depth, not to the whole depth of the numerical model. This will not lead to equilibrium issues and would avoid the overestimation of load capacity, associated with applying the increased value of K_s to the whole depth. For more investigation, simple numerical experiments were conducted by PLAXIS 3D to simulate a micropile in medium-dense sand, with a diameter of 0.2 m and a length of 10 m. The soil behaviour was simulated using the Hardening Soil Model (HS), and its input parameters were determined using the correlations by Brinkgreve et al. [14] (Table 1). The increased value of K_s was applied to the whole width of the model and a variable depth. Figure 3 presents the load-settlement response obtained from the micropile when applying the increased value of K_s in a limited depth (10.2 m) versus the whole depth (20 m). It can be seen that increasing K_s over the whole depth of the numerical model overestimated the load capacity at 25 mm settlement by 17%.

Table 1: Soil input parameters in the numerical model.

Soil	γ	ϕ	ψ	E_{50}^{ref}	E_{oed}^{ref}	E_{ur}^{ref}	P_{ref}	K_s
Sand with increased K_s	17 kN/m ³	34.3°	4.3°	30000 kPa	30000 kPa	90000 kPa	100 kPa	3.0
Sand with original K_s	17 kN/m ³	34.3°	4.3°	30000 kPa	30000 kPa	90000 kPa	100 kPa	0.437

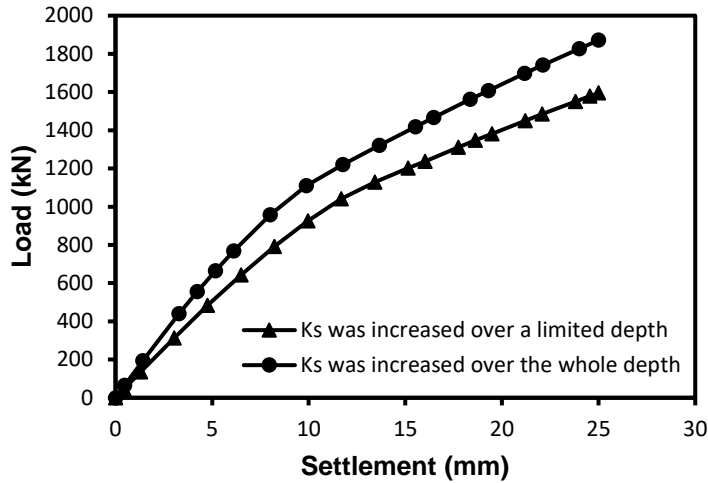


Fig. 3: Effect of the depth of increased K_s on the load-settlement response of micropile.

2.3. The micropile elastic modulus

In comparison to conventional reinforced concrete cast-in-place piles, micropiles generally acquire a high elastic modulus, owing to the high percentage of steel reinforcement utilized in micropiles. In the design of micropiles against lateral loads, the elastic modulus could be a critical parameter. In most cases, micropiles have high slenderness ratios because of their small diameter. Therefore, they will be long enough that the lateral capacity is completely governed by the section's moment capacity (Flexural rigidity). Table 2 presents the reinforcement ratios reported by a number of studies in the literature. It can be seen that the reinforcement ratio in micropiles can be as high as 15.5% of the micropile cross-sectional area.

Table 2: micropile reinforcement ratios from the literature.

Reference	Micropile diameter	Steel reinforcement	Reinforcement ratio
Farouk [7]	0.15 m	3 bars of 32 mm in diameter	13.7%
Kyung et al. [10]	0.165 m	1 bars of 65 mm in diameter	15.5%
Elsawwaf et al. [15]	0.20 m	1 Steel tube with an inner/outer diameter of 76/89 mm	5.4%

In order to properly estimate the micropile elastic modulus, a weighted average can be calculated using the relationship proposed by the FWHA [2]:

$$(1) \quad E_{mp} = (A_{grout} \times E_{grout} + A_{steel} \times E_{steel}) / A_{mp}$$

where E_{mp} is the elastic modulus of the micropile, A_{grout} is the cross-sectional area of the grout, E_{grout} is the elastic modulus of the grout, A_{steel} is the cross-sectional area of the steel, E_{steel} is the elastic modulus of the steel, and A_{mp} is the cross-sectional area of the micropile.

For more investigation, simple numerical experiments were conducted by PLAXIS 3D to simulate two different micropiles: one with a reinforcement ratio of 15% and elastic modulus of 49550 MPa and one with an elastic modulus

of 22000 MPa that is typically used for reinforced concrete. Both micropiles have a diameter of 0.2 m and a length of 10 m. The soil input parameters are shown in Table 1. Figure 4 shows the performance of each micropile for two different loading types: vertical and lateral. It can be seen that the elastic modulus plays an important role in the load capacity. Overlooking the proper estimation of the elastic modulus of a micropile may lead to an underestimated load capacity.

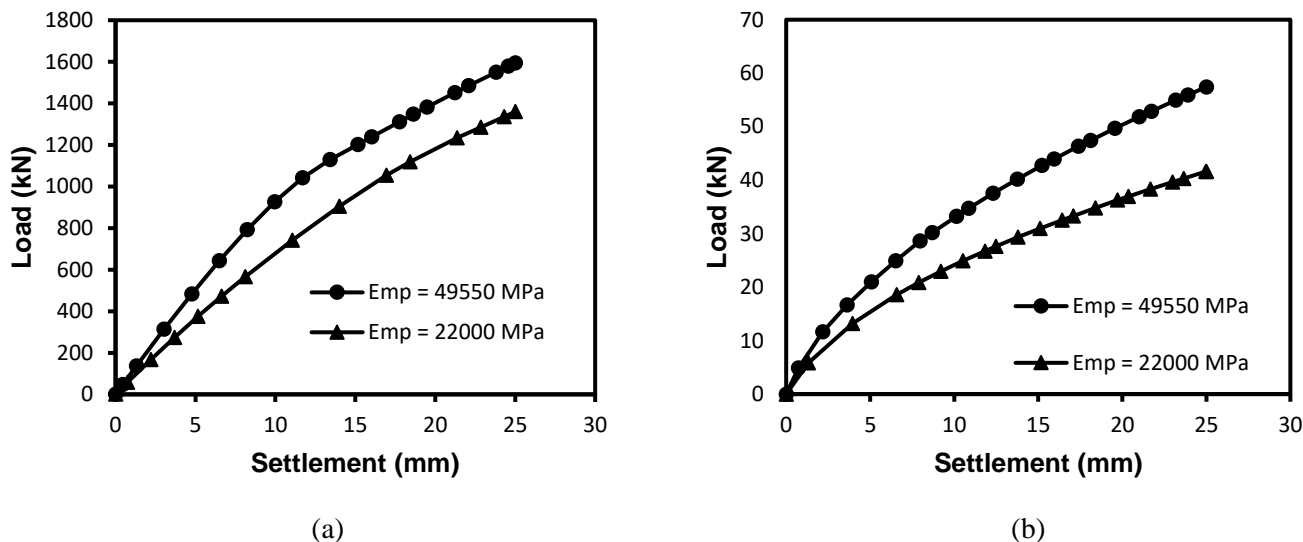


Fig. 4: Effect of E_{mp} on the response of micropile (a) vertical loading (b) lateral loading.

4. Conclusion

1. It is necessary to simulate the micropile installation process or its effects in FE modelling, not to underestimate the micropile load capacity.
2. The interface reduction factor (R_{im}), used to control the friction behaviour of the soil/grout interface, should be in the range of 0.95 to 1.0 to simulate the very rough corrugated surface condition of the micropile.
3. Using an increased value of K_s to simulate the effects of the installation process leads to a non-realistic stress state around the micropile. The increased K_s value should not be applied to the whole depth of the numerical model, not to overestimate the micropile load capacity.
4. In comparison to conventional reinforced concrete cast-in-place piles, micropiles generally acquire a high elastic modulus, owing to the high percentage of steel reinforcement utilized in micropiles. The E_{mp} value should be properly estimated, not to underestimate the micropile performance.

References

- [1] J. S. Moon and S. Lee, "Static skin friction behavior of a single micropile in sand," *KSCE J. Civ. Eng.*, vol. 20, no. 5, 2016, doi: 10.1007/s12205-016-0918-2.
- [2] FHWA, "Micropile Design and Construction Guidelines," *Handbook*, no. 132078, 2005.
- [3] A. M. Alnuaim, H. El Naggar, and M. H. El Naggar, "Performance of micropiled raft in sand subjected to vertical concentrated load: Centrifuge modeling," *Can. Geotech. J.*, vol. 52, no. 1, 2014, doi: 10.1139/cgj-2014-0001.
- [4] A. M. Alnuaim, M. H. El Naggar, and H. El Naggar, "Performance of micropiled raft in clay subjected to vertical concentrated load: Centrifuge modeling," *Can. Geotech. J.*, vol. 52, no. 12, 2015, doi: 10.1139/cgj-2014-0448.
- [5] A. M. Alnuaim, M. H. El Naggar, and H. El Naggar, "Numerical investigation of the performance of micropiled rafts in sand," *Comput. Geotech.*, vol. 77, 2016, doi: 10.1016/j.compgeo.2016.04.002.
- [6] A. M. Alnuaim, M. H. El Naggar, and H. El Naggar, "Performance of micropiled rafts in clay: Numerical investigation," *Comput. Geotech.*, vol. 99, 2018, doi: 10.1016/j.compgeo.2018.02.020.

- [7] A. Farouk, "Behavior of micropiles under vertical tension and compression loads," in *Proceedings of the 17th International Conference on Soil Mechanics and Geotechnical Engineering: The Academia and Practice of Geotechnical Engineering*, 2009, vol. 2. doi: 10.3233/978-1-60750-031-5-1243.
- [8] A. Elsawwaf, A. Nazir, and W. Azzam, "The effect of combined loading on the behavior of micropiled rafts installed with inclined condition," *Environ. Sci. Pollut. Res.*, no. 0123456789, 2022, doi: 10.1007/s11356-022-21327-2.
- [9] A. Elsawwaf, A. Nazir, W. Azzam, and A. Farouk, "The behavior of micropiled raft foundations subjected to combined vertical and lateral loading : numerical study," *Arab. J. Geosci.*, pp. 1–19, 2023, doi: 10.1007/s12517-023-11246-y.
- [10] D. Kyung, G. Kim, D. Kim, and J. Lee, "Vertical load-carrying behavior and design models for micropiles considering foundation configuration conditions," *Can. Geotech. J.*, vol. 54, no. 2, 2017, doi: 10.1139/cgj-2015-0472.
- [11] A. Elsawwaf, M. El Sawwaf, A. Nazir, W. Azzam, A. Farouk, and E. Etman, "Consolidation Effect on the Behavior of Micropiled Rafts Under Combined Loading: Case Study," *Arab. J. Sci. Eng.*, Apr. 2023, doi: 10.1007/s13369-023-07806-9.
- [12] G. Russo, "Full-scale load tests on instrumented micropiles," *Proc. Inst. Civ. Eng. Geotech. Eng.*, vol. 157, no. 3, 2004, doi: 10.1680/geng.2004.157.3.127.
- [13] M. A. Abdlrahem and M. H. El Naggar, "Numerical Modelling of Axial Behaviour of Single and Grouped Hollow Bar Micropiles in Cohesionless Soils," *Geotech. Geol. Eng.*, vol. 41, no. 3, pp. 2105–2126, May 2023, doi: 10.1007/s10706-023-02393-w.
- [14] R. B. J. Brinkgreve, E. Engin, and H. K. Engin, "Validation of empirical formulas to derive model parameters for sands," 2010. doi: 10.1201/b10551-27.
- [15] A. Elsawwaf, M. El Sawwaf, A. Farouk, F. Aamer, and H. El Naggar, "Restoration of Tilted Buildings via Micropile Underpinning: A Case Study of a Multistory Building Supported by a Raft Foundation," *Buildings*, vol. 13, no. 2, 2023, doi: 10.3390/buildings13020422.